Analyst

ROYAL SOCIETY OF CHEMISTRY

PAPER

View Article Online
View Journal | View Issue

Cite this: *Analyst*, 2022, **147**, 614

Rapid detection of airborne protein from *Mycobacterium tuberculosis* using a biosensor detection system†

Jinbiao Ma, ‡[a,b] Guanyu Jiang,‡[a,b] Qingqing Ma,[e] Hao Wang,[c,f] Manman Du,[a,b] Can Wang, *[a,b] Xinwu Xie, *[c,d] Tie Li[g,h] and Shixing Chen[g,h]

Tuberculosis (TB), caused by infection with airborne *Mycobacterium tuberculosis* (MTB), seriously threatens human health and has become a public health problem of worldwide concern. To achieve effective control of TB, rapid and sensitive detection of MTB is particularly important. At present, the common detection methods for MTB cannot meet the requirements of speed, flexibility and portability simultaneously. In this work, a multichannel microfluidic chip was developed and packaged with an ultra-sensitive silicon nanowire field-effect-transistor biosensor. The fluid system was tested and optimized through simulation, and the best conditions were determined: the flow rate was 0.3 mL min^{-1} and the flow direction was perpendicular to a silicon nanowire. A one-way valve, a switching valve and a peristaltic pump were combined to establish a biosensor detection system to realize the automatic detection of TB samples. Then we systematically explained the factors affecting simulated exhaled breath condensate (SEBC) collection, and established and optimized the method for collection of SEBC from the perspective of collection volume and biological activity. The best collection conditions were determined for a 5 mm pipe diameter at 0 °C, and a sufficient sample volume was obtained in only 2 minutes for microfluidic detection. Then, the actual application value of the established collection method was further evaluated. Volunteers were recruited and this method was used to collect their exhaled breath condensate to analyze the collection effect. The system detected MTB in SEBC with good sensitivity (~4×10^4 particles per mL). It is expected to be further integrated and miniaturized in the future to realize point-of-care testing.

Received 21st November 2021,
Accepted 13th January 2022

DOI: 10.1039/d1an02104d

rsc.li/analyst

1. Introduction

Infection with tuberculosis (TB) is caused by the spread of airborne *Mycobacterium tuberculosis* (MTB). When an infected person coughs, speaks, spits or sneezes, MTB is released into the environment and spreads through aerosols.[1,2] MTB has a strong resistance to harsh environments and can survive for a long time in aerosols. The continuation of the TB epidemic is driven by successive cycles of infection, lung disease, bioaerosol excretion of MTB and inhalation by susceptible individuals. Therefore, rapid and accurate detection of TB is the basis for TB control.[3] Rapid, efficient, effective and low-cost detection of MTB is a challenge facing scientists all over the world. At this stage, the conventional detection methods for MTB include the culture method, imaging detection, sputum smear microscopy, the PPD experiment, serological detection and molecular diagnosis.[4,5] However, most of these technologies are usually limited by the need for a sample to be collected and analyzed in a laboratory environment. The detection process is complicated and time-consuming and has high operation requirements, and it is difficult to meet the actual detection needs of MTB.[6]

[a]*School of Environmental Science and Engineering, Tianjin University, Tianjin, 300072, PR China. E-mail: wangcan@tju.edu.cn*
[b]*Tianjin Key Lab of Indoor Air Environmental Quality Control, Tianjin, 300072, PR China*
[c]*Institute of Medical Support Technology, Academy of Military Science, Tianjin, 300161, PR China. E-mail: xinwuxie@163.com*
[d]*National Bio-Protection Engineering Center, Tianjin, 300161, PR China*
[e]*Department of Respiratory Medicine, Shandong Public Health Clinical Center (Shandong Province Chest Hospital), Jinan, 250013, PR China*
[f]*School of Electronic Information and Automation, Tianjin University of Science and Technology, Tianjin, 300222, PR China*
[g]*Science and Technology on Micro-System Laboratory, Shanghai Institute of Microsystem and Information Technology, Chinese Academy of Sciences, Shanghai 200050, PR China*
[h]*State Key Laboratories of Transducer Technology, Shanghai Institute of Microsystem and Information Technology, Chinese Academy of Sciences, Shanghai, 200050, PR China*

†Electronic supplementary information (ESI) available. See DOI: 10.1039/d1an02104d

‡These authors contributed equally to this work.

Nowadays, non-invasive methods are a good choice for TB diagnosis. As a commonly available non-invasive sampling method, exhaled breath samples are considered an attractive strategy, mainly collecting non-volatile molecules in the patient's exhaled breath, including small molecules, lipids and proteins.[7] The mixture contained in breath is not as complicated as those in sputum, serum and urine, and can be used for screening, early auxiliary diagnosis and disease monitoring of TB.[8,9] It has been confirmed that there is cultivable MTB in the exhaled breath of TB patients and it is feasible and reproducible to collect exhaled breath for detection.[10] Collecting exhaled breath condensate (EBC) is a common method for exhaled breath sample collection. EBC collection relies on the existence of a temperature gradient between the hot and high-humidity exhaled air and the cold collection structure, so that the exhaled air can be condensed and collected as a liquid for analysis.

The EBC collection method has advantages because it only requires tidal energy to breathe and does not require an external air pump and the sample is easy to obtain. However, the current collection method of EBC has not yet been standardized. Under normal circumstances, young people can collect 1–3 mL EBC in 10 minutes of tidal breathing. It is worth noting that the EBC collection volume could be affected by many factors, such as the condensing temperature and time, the collection flow rate and the basic characteristics of the subject (such as age, gender, vital capacity and smoking status).[11] At present, there is a lack of standard methods for EBC collection and the assessment of biological activity in EBC, and many related studies are urgently needed. Xu *et al.* designed a simple condensation sampler based on condensation collision, which can collect 100 μL of EBC within 2 min. However, the device uses a narrow-diameter suction tube for oral test sample collection, which is not conducive to the patient maintaining continuous steady-state breathing.[12]

Moreover, the real-time detection of MTB in air is difficult, and several factors complicate it. Perhaps the most challenging obstacle is the extremely low levels of particles found in aerosols, making detection difficult for common detection methods owing to their low sensitivity.[13,14] Biosensor technology development is relatively mature, and it has the advantages of high integration, high sensitivity and short detection time.[15] Many existing air samplers are not very effective collectors, resulting in additional loss of captured pathogens and making it difficult to detect them. Mcdevitt *et al.* designed the G-II EBC collector to distinguish the different types of EBC produced by the oral cavity and respiratory tract. However, this sampler collects by collision and settlement, which has a low collection efficiency and high loss, making it unsuitable for practical applications.[16] Therefore, in order to perform a sufficiently sensitive detection, an optimal air sampler parameter must be found to capture as much aerosol as possible for accurate sampling.[17]

The next problem to be solved is how to connect the microorganisms captured by the above method and the interface of the actual detection device. Sousa *et al.* developed an electrostatic air sampler to collect cough samples from TB patients. However, the collected samples require DNA extraction and amplification to complete the test, which is quite time consuming.[18] In our previous study,[19] the silicon nanowire field-effect-transistor (SiNW-FET) biosensor as an ultra-sensitive detection technology could detect 33aM MTB samples, and the shortest response time was 30 s. The specificity and stability of the sensor have been tested in detail, and good results have been achieved. Compared with other molecular, immune and sensor detection technologies, our biosensor can detect MTB Ag85B protein with a wider concentration range in a shorter time.[20] However, the sample usually requires manual labor to load it onto the actual sensor for detection, which will cause errors.[15] Moreover, since MTB is mostly transmitted through air, it is not enough to detect only liquid TB samples. Therefore, a continuous sampling system that can automatically load captured airborne TB samples into sensors should be established.

In order to improve the efficiency of the experiment, the microfluidic system came into being. Compared with other analysis technologies, the microfluidic chip flexibly combines multiple operating units, showing the unique advantages of system integration, equipment miniaturization, portability, automation of the operation process, low reagent consumption, the elimination of man-made interference, pollution prevention, ease of integration with other technical equipment and good compatibility.[21,22] The above-mentioned characteristics of the microfluidic chip make the experiment of the chip concept into a reality.[23,24] This shift from a traditional central laboratory to a chip experiment has brought revolutionary progress for many researchers. Work that originally needed to be done in a laboratory can now be done on a chip.[25,26] Shen *et al.* developed a sensor for the real-time detection of H3N2 influenza virus by integrating electrostatic air sampling, microfluidics and SiNW-FET biosensors. However, static air sampling is not easy to charge, so it cannot effectively capture the virus.[27]

In this work, we developed a multichannel microfluidic chip with an ultra-sensitive SiNW-FET biosensor to detect MTB. The fluid system was simulated to get the best flow conditions. We systematically explained the factors that affect the simulated exhaled breath condensate (SEBC) collection. Then we established and optimized the collection method of SEBC from the perspective of collection volume and biological activity. Then the actual application value of the established collection method was further evaluated. We recruited volunteers and used the above method to collect their EBC to analyze the collection effect. Combined with a one-way valve, a switching valve and a peristaltic pump, a SiNW-FET biosensor detection system for actual samples of nodules was established. The system can reduce the errors caused by human operation, and reduce the number of samples, and the detection can be completed without the need for professionals. The system is expected to realize the preliminary screening of TB patients through EBC detection and provide new ideas for ending TB.

2. Materials and methods

2.1. Materials

An LM60B peristaltic pump, a switching valve, a one-way valve and a piping system were purchased from Runze Fluid (Nanjing, China). The EBC collector bioscreenII was purchased from Dinglan (Beijing, China). The aerosol generator ATM-226 was purchased from Topas (Germany). The gas mass flow meter CAFS5008B was purchased from Consensic (USA). The Coriolis Micro Bio-Aerosol Sampler was from Bertin (France). The optical particle size spectrometer was purchased from TSI (USA). The MTB Ag85B protein and anti-Ag85B were purchased from Abcam (USA). The MTB Ag85B ELISA Kit was bought from Meimian (Jiangsu, China).

2.2. Optimization of SEBC acquisition parameters

In order to explore influencing factors in the collection of EBC and determine the best operating parameters for practical application, we used the method of controlling variables to explore the effects of various factors on the SEBC collection effect, including the diameter of the gas pipe, the volume of aerosol passing through the condenser and the condensation temperature. In this experiment, the aerosol generator stock solution used was the simulated SEBC formulated according to the physical composition of SEBC (Table S1†). We screened for the experimental methods with the highest efficiency and the lowest energy consumption (including the diameter of the gas pipe, the condensation temperature and the collection volume) using the test in Fig. S1(a).†

Then, we recruited volunteers for practical application tests, as shown in Fig. S1(b).† We recruited 5 males and 5 females from Tianjin University, a total of 10 volunteers aged 22–24, with no smoking history and no respiratory diseases. A picture of the device is shown in Fig. S2.† A picture of volunteers using the equipment for SEBC collection is shown in Fig. S3.† Under the best experimental conditions, the application results for volunteers were recorded to evaluate the feasibility of the combination of the condensation collection method and the subsequent microfluidic technology.

In addition, we further explored the influence of condensation temperature on microbial activity in SEBC owing to the higher requirements for microbial activity. In this experiment, we used an *E. coli* suspension as the aerosol generator stock solution. As shown in Fig. S1(c),† we used plate culture and flow cytometry to analyze the cultivable performance and cell morphology of microorganisms in SEBC at different condensation temperatures, respectively. Then, we used the same analysis method to explore the biological activity in the actual SEBC of volunteers, in order to evaluate sensor protein detection scientifically from the perspective of biological activity. The error bars for all of the data in this study were calculated using the STDEVA function in Excel for three independent experiments.

2.3. Preparation of biosensors and integration of microfluidic chips

The 360-SiNWs array was prepared following the "top-down" method, including chemical vapor deposition, lithography, anisotropic etching, self-limiting oxidation and a doping process on a (111) SOI wafer.[19] Then boron was doped at the designed electrode position to form a good ohmic contact between the silicon and the metal electrode. Then it was packaged on the printed circuit board to complete the preparation of the SiNW-FET biosensor. As shown in Fig. 1(a), the packaged biosensor is flexible and portable (36 × 31 mm). A scanning electron microscope was used to characterize the different dimensions of the biosensor surface. As shown in Fig. 1(b), Au was used as the contact metal and for leading wires. The deposition of TiW/Au as electrodes was done using a doping process with ions injected at defined locations to form ohmic contacts. 360 well-ordered SiNWs were arranged on a chip as a sensing element. The SiNW on the inner wall of the pit was in a suspended state and the surface was covered with an oxide layer. The SiNW was a conductive channel hidden underneath the Au and silicon nitride layers and could not be directly observed. As shown in Fig. 1(c), SEM was used to characterize the oxide layer on the etched SiNW surface and revealed that its width was small at only 73.7 nm. Given that the SiNW with a small diameter has a large surface-to-volume ratio, the dimension of the NWs will play an important role in the transport properties.

We used SOLIDWORKS software for the design and used a laser engraver to etch a transparent plastic polymethyl methacrylate (PMMA) microfluidic chip to achieve the integration of the above-mentioned biosensors. The PMMA material had good light transmittance and could be visually observed on the liquid path system. A schematic and a physical diagram after combining the multichannel microfluidic pipelines are shown in Fig. 1(d). Fig. 1(e) shows the detailed structure of the multichannel microfluidic chip, including the multichannel pipe upper chip, the microfluidic cavity middle chip and the SiNW-FET biosensor lower chip. The three parts were bonded using 707 glue. First, the upper chip and the middle chip were aligned, and then glue was applied along the edge of the gap and allowed to dry naturally for 15 min to achieve airtightness. Then the glue was carefully smeared along the periphery of the microfluidic cavity of the middle chip (to avoid flow into the reaction chamber that would affect detection), the integrated microfluidic chip was aligned with the biosensor using the fixed column and the preparation was completed by natural drying for 15 min. The upper chip contained eight microtubes and an external one-way valve made the microtubes seven in and one out, ensuring one-way flow of the fluid system without cross-contamination. Each microtube had a 0.9 × 0.3 mm microfluidic channel that was transported to the middle chip. The middle layer microfluidic chip had two 0.9 mm-diameter through holes and a 0.3 × 1.3 × 1.6 mm microfluidic cavity with round-cut corners was set in it for biological reactions. Following the method of Shen *et al.*,[28] we used norepinephrine bitartrate monohydrate as a surface modifier to increase the hydrophilicity of the microfluidic chip. We measured the hydrophilic angle of PMMA before and after modification. As shown in Fig. S4,† the hydrophilicity increased after modification. This made the injection and flow of the aqueous solu-

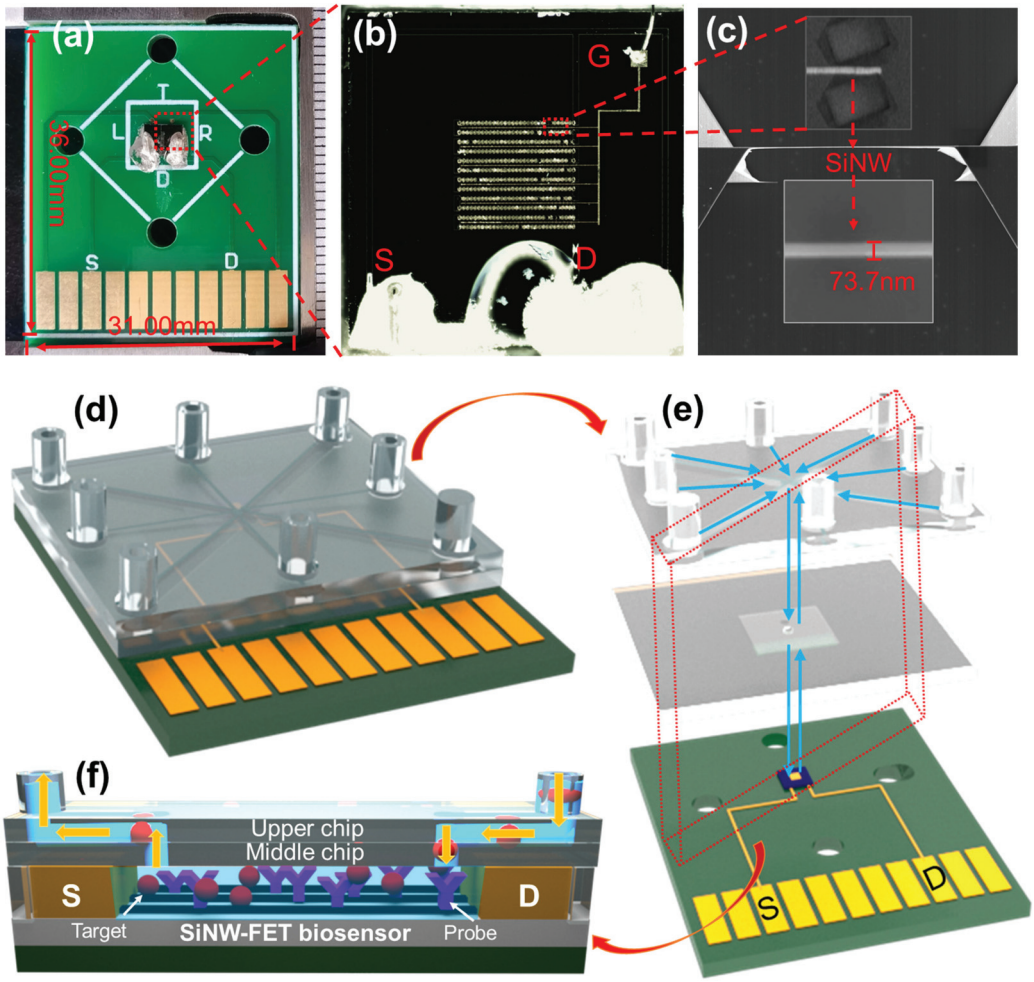

Fig. 1 Design of microfluidic chip biosensor. (a) Image of the packaged device; (b) optical microscope image of 360-SiNWs array; (c) SEM of SiNW; (d) microfluidic chip assembly drawing; (e) exploded view of microfluidic chip; and (f) microfluidic chip detection principle.

tion more convenient and improved the performance of biochemical analysis of the microfluidic chip.

As shown in our previous investigation, the Ag85B protein is a secreted protein of MTB. It is abundant on the surface of MTB, so it can be used as a simulant of MTB.[29,30] We performed surface functionalization on the prepared sensor. First, the surface of the sensor was treated with oxygen plasma, and then the above packaging method was used to encapsulate the microfluidic chip biosensor. Then the previous method was followed to functionalize the sensor.[19] The detection principle of the multichannel microfluidic chip biosensor is shown in Fig. 1(f). First, the TB-specific substance Ag85B antibody is fixed to the surface of the biosensor,[19] and the airborne protein from MTB is converted into a liquid sample using the method of condensation collection. Then the liquid sample to be tested is injected into the microfluidic chip biosensor and flows through the channels of the upper chip and the middle chip to the microfluidic cavity. Dynamic flow of the sample is maintained throughout the detection process, which greatly improves the capability of the biological analysis.[31] When the TB sample containing the target (MTB Ag85B protein) enters the microfluidic cavity, the surface of the biosensor with the probe (MTB Ag85B antibody) fixed will have specific binding. The SiNW-FET biosensor can sensitively respond to the tiny electrical signals generated to complete the detection.

2.4. Construction of the detection system

The process of the entire SiNW-FET biosensor detection system is shown in Fig. 2. The peristaltic pump is connected to the sample collection device to realize real-time sample injection. Then the peristaltic pump is connected to the multichannel switching valve to realize the multichannel liquid path selection. Then a one-way valve is connected to prevent backflow of the liquid path and ensure that the sample is not contaminated. Then the packaged multichannel microfluidic chip is connected, as well as the electrochemical detection equipment and the signal display device, and the construction of the automated multichannel microfluidic biosensor detection system is completed. According to the requirements of the experiment, each sample can be analysed sequentially or in

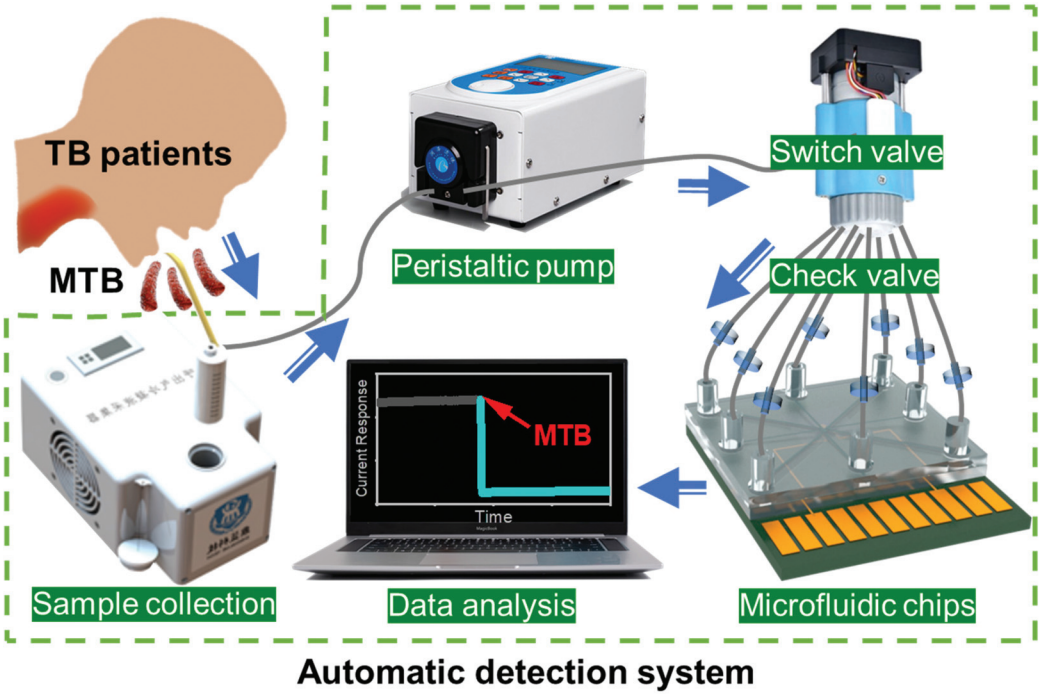

Fig. 2 Diagram of the biosensor detection system for EBC.

parallel. On the microfluidic chip, the interference of the sample and the concentration can also be reduced. A picture of the device is shown in Fig. S5.† We tested the liquid path system of the detection system using different concentrations of PBS buffer solution. As shown in Fig. S6,† the switching valve was used to switch different samples in sequence, and the detection system can have a sensitive response.

3 Results and discussion

3.1. Optimization analysis of SEBC acquisition parameters

The overall SEBC acquisition parameter optimization process is shown in Fig. 3. As shown in Fig. 3(a), as the inner diameter of the air pipe increases, the collection volume of the exhaled aerosol gradually decreases. When the inner diameter of the air pipe increases from 2 to 8 mm, the collection effect at 10 min decreases by 20%. At a certain flow rate, the gas flow rate is inversely proportional to the square of the pipe diameter, as shown in eqn (1):

$$Q = \frac{\pi}{4} \cdot V \cdot D^2 \quad (1)$$

where Q is the flow rate in the gas pipe (L min^{-1}), V is the flow velocity in the gas pipe (m s^{-1}) and D is the inner diameter of the gas pipe (mm).

The SEBC volume gradually increases but the growth rate gradually decreases as the aerosol flow rate increases. This may be due to the fact that the increase in the flow rate brings in more aerosol particles per unit time, but reduces the residence time of the aerosol in the condenser tube. In addition, higher flow rates will take away or evaporate some of the small droplets that have been condensed. In addition, the actual experience of the subjects should also be considered, which is directly related to the pipe resistance. The calculation of the pipe resistance is shown in eqn (2):

$$R = \frac{\lambda}{D} \cdot \frac{V^2 \cdot \gamma}{2g} \quad (2)$$

where R is the friction resistance (kgf m^{-2}), λ is the drag coefficient, γ is the fluid density (kg m^{-3}) and g is the acceleration due to gravity.

The determination of the drag coefficient λ is shown in Table S2.† Excessive friction resistance was not conducive to the subject adopting a smooth mouth-breathing method for SEBC collection. On the whole, we selected a silicone gas pipe with an inner diameter of 5 mm for research and application.

As shown in Fig. 3(b), taking 0 °C as the separation temperature, when the same volume of aerosol was introduced, there was no significant difference in the SEBC volume under the condensation conditions −10, −5 and 0 °C. The SEBC collection effect under the 5 and 10 °C condensing conditions was 13 and 30% lower than the average levels at −10 and 0 °C, respectively. According to the liquid film rupture hypothesis, the phase interface temperature difference of heat transfer during condensation collection is mainly provided by zero-degree droplets and hot exhaled breath.[32] Therefore, choosing 0 °C as the condensing temperature can save energy and achieve better SEBC collection efficiency in practical applications.

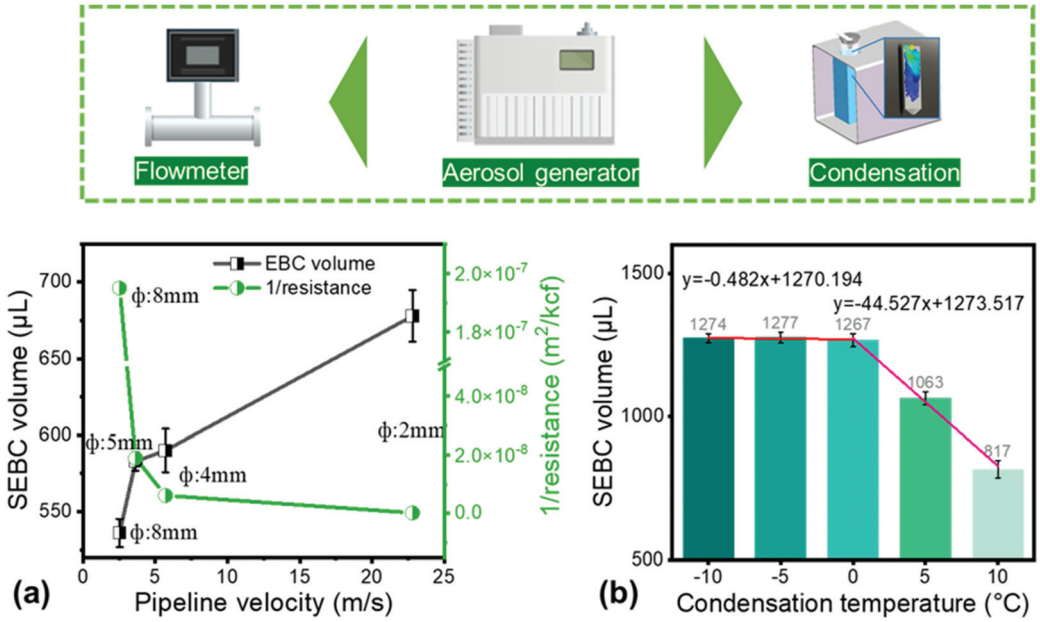

Fig. 3 Establishment and optimization of exhaled breath condensation collection method. (a) Influencing results for pipe diameter. (b) Influencing results for condensation temperature. Each data set displays the average and the SD of the results from three independent experiments (n = 3).

3.2. Microbial activity exploration and practical application evaluation

We used the plate culture test to analyze the *E. coli* condensate collected at different condensation temperatures, and there was no significant difference in concentration (Fig. S7†). The flow cytometry analysis results for SEBC are shown in Fig. S8(a)–(f).† There was no significant difference in the survival status of *E. coli* at different condensation temperatures, which is consistent with the trend obtained by the plate

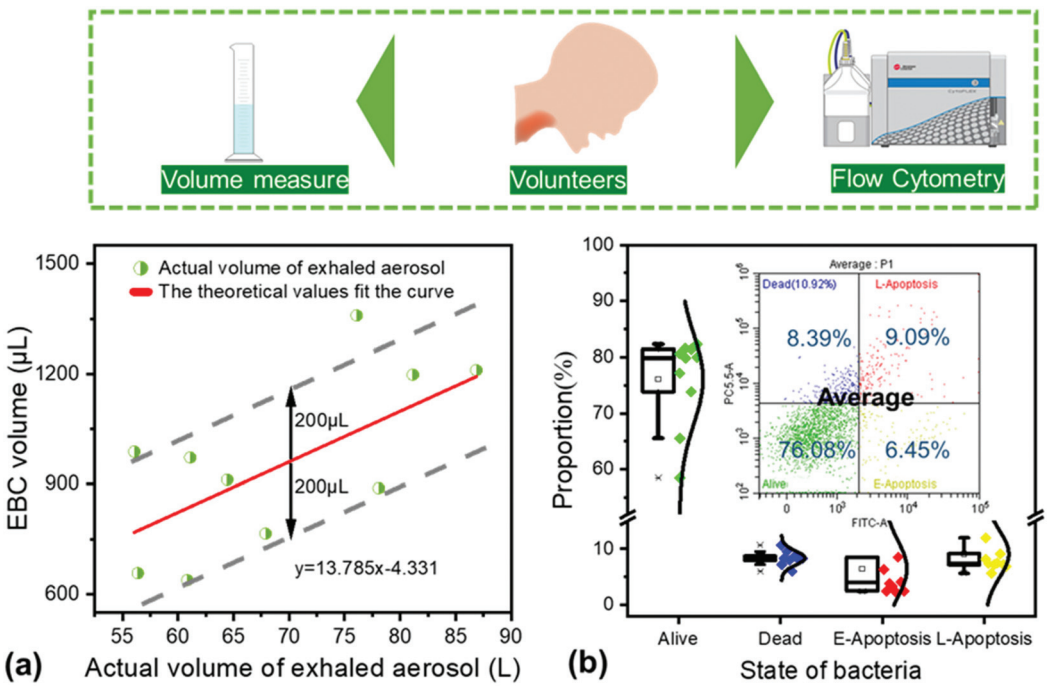

Fig. 4 Application evaluation for recruiting volunteers. (a) The relationship between the actual exhaled air volume and the EBC volume of volunteers (compared with the experimental fitting curve). (b) The survival status of microorganisms in the actual EBC of volunteers.

culture method. This can be explained by the fact that most bacteria contain cold shock protein, so they can adapt to low-temperature environments.[33–35] This shows that the condensation collection method has a high capture efficiency for microbial components in the aerosol, and at the same time can achieve the enrichment of the exhaled aerosol microorganisms under the premise of ensuring the reproduction ability of the cultivable microorganisms.[36,37]

As shown in Fig. S9,† we fitted a linear relationship between the exhaled air volume and the SEBC volume at 0 °C, and its R^2 was 0.99, indicating that there is a strong linear correlation between them. The research results of Gessner *et al.* also reached a similar conclusion.[38] Furthermore, we recruited 10 volunteers and collected their exhaled breath for 10 minutes, and then recorded their exhaled breath volume and EBC collection volume during 10 minutes. The results of comparing their exhaled aerosol volume–EBC volume with the fitted curve are shown in Fig. 4(a). The EBC collected under the corresponding exhaled aerosol volume steadily fluctuated within an error range of 0.2 mL from the theoretical calculation value. This shows that the aerosol volume flow–EBC volume model established in this experiment has good practical application value. In practical applications, the acquisition time can be reasonably controlled according to the amount of EBC required. For microfluidic detection, a sufficient sample volume of 175 μL can be obtained in only 2 minutes, as shown in Fig. S9.†

Finally, we used flow cytometry to analyze the biological activity of EBC in 10 volunteers, as shown in Fig. 4(b). The median proportion of live cells in volunteer EBC was about 80%. The condensation collection method can better maintain the microbial morphology in the respiratory tract and can ensure the accuracy of subsequent biological detection, which means that the system error of the EBC condensation collection method is small and the damage ratio of living cells during the condensation collection process is stable. In summary, the EBC condensation collection method is easy to repeat and has good practical application value in subsequent testing.

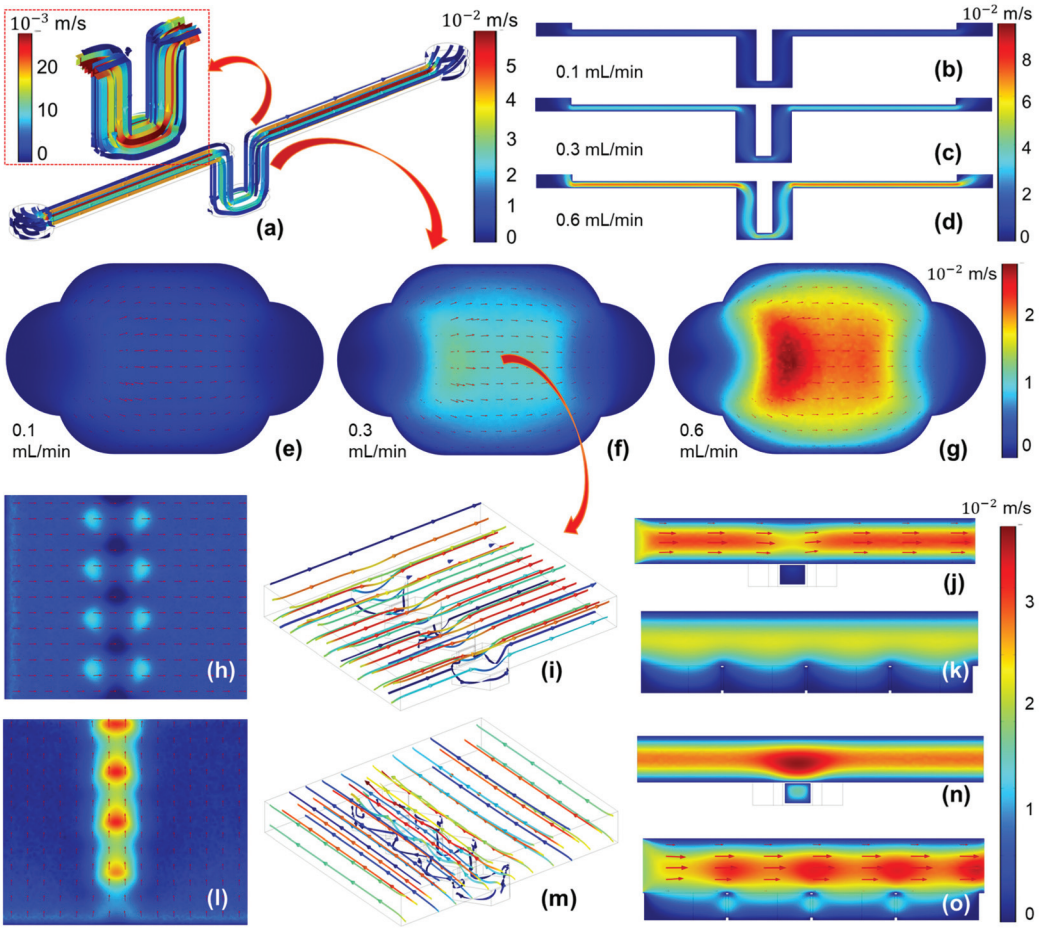

Fig. 5 Fluid system simulation. (a) The streamline and velocity simulation and enlarged detail of microfluidic chip; front view of the microfluidic chip velocity simulation under the liquid flow rates of (b) 0.1 mL min^{-1}, (c) 0.3 mL min^{-1} and (d) 0.6 mL min^{-1}; top view of the microfluidic chip velocity simulation under the liquid flow rates of (e) 0.1 mL min^{-1}, (f) 0.3 mL min^{-1} and (g) 0.6 mL min^{-1}; (h) top view of SiNW velocity simulation with flow direction parallel to SiNW; (i) streamline simulation of SiNW with flow direction parallel to SiNW; flow velocity simulation of (j) SiNW profile and (k) pit profile with flow direction parallel to SiNW; (l) top view of SiNW velocity simulation with flow direction perpendicular to SiNW; (m) streamline simulation of SiNW with flow direction perpendicular to SiNW; flow velocity simulation of (n) SiNW profile and (o) pit profile with flow direction perpendicular to SiNW.

3.3. Fluid system simulation

Control of the sample flow is key to the development of a microfluidic integrated biosensor and the improvement of bioanalysis capabilities.[31] Therefore, it was necessary to simulate the flow rate of the microfluidic chip. We used COMSOL software to simulate a single-channel fluid system under ideal conditions. The simulation parameters were set as follows: fluid density was 1000 kg m^{-3}; hydrodynamic viscosity was 1.003×10^{-3} N S m^{-3}; outlet pressure was 0 Pa; and the fluid was an incompressible fluid with no wall slippage, ignoring wall tension. As shown in Fig. 5(a), the streamline and velocity distribution in the fluid system basically meet the requirements of automatic sampling. Then we used three flow rates of 0.1, 0.3 and 0.6 ml min^{-1} to test the best conditions of the fluid system. The specific front view can be seen in Fig. 5(b)–(d) and the top view can be seen in Fig. 5(e)–(g). It can be seen that the flow rate distribution is most stable under the condition of 0.1 mL min^{-1}, but the flow rate is too low and requires high accuracy of the peristaltic pump and the slow sample delivery speed affects the rapid detection. However, the flow velocity distribution is uneven at 0.6 mL min^{-1}, which may cause turbulence that may damage biological macromolecules and affect specific detection. It can be seen that the liquid path system with a flow rate of 0.3 mL min^{-1} is the most stable and can meet the requirements for use. Therefore, we chose 0.3 mL min^{-1} as the injection flow rate.

SiNW exists on the tangent line of the hexagonal groove, and its suspended microstructure determines the direction of liquid flow that will have the greatest influence on the distribution of its fluid parameters. Based on the inlet flow rate of 0.3 mL min^{-1}, we simulated the influence of the flow direction of the solution relative to the SiNW on the distribution of liquid path parameters. Fig. 5(h)–(k) shows simulations with a flow direction parallel to the SiNW. Fig. 5(l)–(o) shows simulations with a flow direction perpendicular to the SiNW. Compared with the flow direction parallel to SiNW, it can be seen that the liquid still keeps flowing in the pit when it is perpendicular to the SiNW direction, which is conducive to biospecific recognition. At the same time, this flow direction can

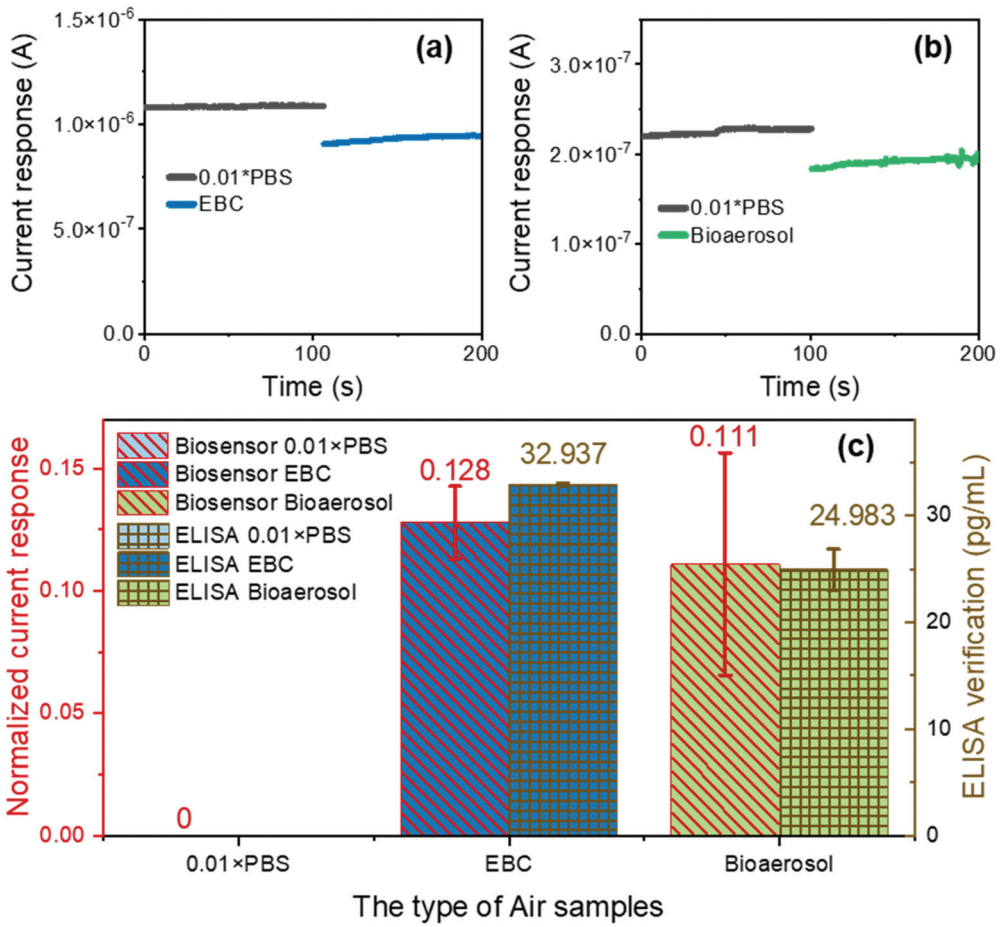

Fig. 6 The detection system specifically recognizes the air samples. (a) The detection system detects the real-time current response of concentration gradient MTB Ag85B protein in bioaerosol; (b) the detection system detects the real-time current response of concentration gradient MTB Ag85B protein in exhaled breath simulant; (c) the detection system detects the normalized current response of concentration gradient MTB Ag85B protein in air samples. Each data set displays the average and SD of the results from three independent experiments (n = 3).

quickly change the solution around the SiNW when switching the sample as there is no dead volume, thereby shortening the response time of the biosensor. Therefore, we chose a flow direction perpendicular to the SiNW.

3.4. Air sample testing

In order to test the system, a six-nozzle Collison sprayer (BGI CN31l) was used for aerosol generation of MTB Ag85B protein at a pressure of 7.6 bar, and a high-pressure air filter was connected to ensure that there were no other impurities. Fennelly *et al.* proved that tuberculosis patients can produce particles with an aerodynamic diameter of 0.65–3.3 μm.[39] The optical particle size spectrometer (TSI 3330) was used to test the particle size distribution in this study. Its aerodynamic diameter is concentrated between 0.3 and 4.16 μm, and the concentration is 4×10^4 particles per mL, which can be used to simulate high concentrations of EBC. First, patient exhalation simulation was performed (Fig. S10†), the outlet of the nebulizer was connected to the EBC collector bioscreenII to collect the SEBC, and it was collected for 10 minutes at 0 °C. It was continuously transmitted to the microfluidic chip through a peristaltic pump at a control flow rate of 0.3 mL min^{-1}, and connected to the signal acquisition system for detection. The detection results for aerosol volatilization of the PBS buffer and 10 ng mL^{-1} MTB Ag85B protein are shown in Fig. 6(a). The response can distinguish PBS buffer and TB simulated exhaled breath well. It is proved that the system can achieve a sensitive response to SEBC.

At the same time, we explored simulated environmental aerosols to provide early warning of high concentrations of MTB aerosols in TB aggregation sites (Fig. S11†). The results are shown in Fig. 6(b). The current response can distinguish PBS buffer and TB simulated environmental aerosols well. It is proved that the system can achieve a sensitive response to environmental aerosol samples. As shown in Fig. 6(c), we normalized the above data, and it can be seen that the automatic microfluidic detection system can achieve the initial measurement of environmental air samples and show good sensitivity (>0.1). Compared with EBC, the bioaerosol data have a larger error bar. The reason for this may be that bioaerosol sampling is more likely to collect impurities in the air environment into the sample owing to its cyclone collection principle. Related aerosol samples and SEBC samples were qualitatively verified using ELISA, and the values were 24.98 and 32.93 pg mL^{-1}, respectively. The signal detected by the system is positively correlated with the above values and is expected to achieve the initial quantitative detection of air samples. While more data is needed to confirm the feasibility of using this biosensor in real-world air sample testing, we certainly present a new idea that could be applied for rapid preliminary screening of TB patients.

4. Conclusion

In this research, we successfully designed and fabricated a multichannel microfluidic chip to connect with an ultra-sensitive SiNW-FET biosensor. The fluid system was simulated to obtain the best injection conditions of 0.3 mL min^{-1} flow rate and flow direction perpendicular to the SiNW. Combining a one-way valve, a switching valve and a peristaltic pump, a FET biosensor detection system for actual samples of nodules was integrated. The system can reduce errors caused by human operation and reduce the number of samples, and the detection can be completed without the need for professionals. The microorganism was verified to maintain good activity under the optimal air sample collection conditions of 5 mm pipe diameter and 0 °C condensation temperature. For microfluidic detection, a sufficient sample volume can be obtained in only 2 minutes. The system can detect protein from MTB in SEBC ($\sim 4 \times 10^4$ particles per mL), verifying the feasibility of the microfluidic system. The microfluidic device can be used not only for the detection of actual TB samples, but also for the detection of other airborne pathogenic bacteria. This method provides an effective method for the direct and rapid detection of other pathogens on the microfluidic chip, and also provides the possibility for early warning of the spread of infectious diseases. At the same time, the microfluidic chip also provides the possibility of automation or integration with existing analysis systems.

Author contributions

J. M. conceived the study, designed and performed experiments, analyzed data, and wrote the manuscript. G. J. performed experiments in SEBC acquisition, and wrote the manuscript. C. W. and X. X. conceived the study, obtained funding, and revised the manuscript. Q. M. revised the manuscript. H. W. and M. D. supervised the work, coordinated the collaborations. T. L. and S. C. designed the biosensor. All authors have given approval to the final version of the manuscript.

Conflicts of interest

The authors declare that they have no known competing financial interests or personal relationships that could have appeared to influence the work reported in this paper.

Acknowledgements

This research was supported by the Key Technologies R & D Program of Tianjin (20ZXGBSY00100), National Natural Science Foundation of China (grant no. 51678402) and National Science and Technology Major Project (2017ZX10304403-003-004).

All experiments were performed in accordance with the relevant laws, guidelines and institutional guidelines, and approved by the ethics committee at Tianjin University. Informed consents were obtained from human participants of this study.

References

1 C. C. Wang, K. A. Prather, J. Sznitman, J. L. Jimenez, S. S. Lakdawala, Z. Tufekci and L. C. Marr, Airborne transmission of respiratory viruses, *Science*, 2021, **373**, 981, DOI: 10.1126/science.abd914.

2 G. Jiang, C. Wang, L. Song, X. Wang, Y. Zhou, C. Fei and H. Liu, Aerosol transmission, an indispensable route of COVID-19 spread: Case study of a department-store cluster, *Front. Environ. Sci. Eng.*, 2021, **15**, 46, DOI: 10.1007/s11783-021-1386-6.

3 World Health Organization, Global Tuberculosis Report, 2020, https://www.who.int/teams/global-tuberculosisprogramme/data (update 14 October 2020).

4 J. Furin, H. Cox and M. Pai, Tuberculosis, *Lancet*, 2019, **396**, 1642–1656, DOI: 10.1016/S0140-6736(19)30308-3.

5 K. Rizi, E. Aryan, Z. Meshkat, G. Ranjbar, M. Sankian, K. Ghazvini, H. Farsiani, H. R. Pourianfar and M. Rezayi, The overview and perspectives of biosensors and Mycobacterium tuberculosis: A systematic review, *J. Cell. Physiol.*, 2021, **236**, 1730–1750, DOI: 10.1002/jcp.30007.

6 S. Gupta and V. Kakkar, Recent technological advancements in tuberculosis diagnostics – A review, *Biosens. Bioelectron.*, 2018, **115**, 14–29, DOI: 10.1016/j.bios.2018.05.017.

7 F. Shen, J. Wang, Z. Xu, Y. Wu, Q. Chen, X. Li, X. Jie, L. Li, M. Yao, X. Guo and T. Zhu, Rapid flu diagnosis using silicon nanowire sensor, *Nano Lett.*, 2012, **12**, 3722–3730, DOI: 10.1021/nl301516z.

8 B. Patterson, A. Koch, S. Gessner, R. Dinkele, M. Gqada, W. Bryden, F. Cobelens, F. Little, D. F. Warner and R. Wood, Bioaerosol sampling of patients with suspected pulmonary tuberculosis: a study protocol, *BMC Infect. Dis.*, 2020, **20**, 587, DOI: 10.1186/s12879-020-05278-y.

9 E. C. Jones-López, C. Acuña-Villaorduña, M. Ssebidandi, M. Gaeddert, R. W. Kubiak, I. Ayakaka, L. F. White, M. Joloba, A. Okwera and K. P. Fennelly, Cough aerosols of *Mycobacterium tuberculosis* in the prediction of incident tuberculosis disease in household contacts, *Clin. Infect. Dis.*, 2016, **63**, 10–20, DOI: 10.1093/cid/ciw199.

10 K. P. Fennelly, E. C. Jones-Lopez, I. Ayakaka, S. Kim, H. Menyha, B. Kirenga, C. Muchwa, M. Joloba, S. Dryden-Peterson, N. Reilly, A. Okwera, A. M. Elliott, P. G. Smith, R. D. Mugerwa, K. D. Eisenach and J. J. Ellner, Variability of infectious aerosols produced during coughing by patients with pulmonary tuberculosis, *Am. J. Respir. Crit. Care Med.*, 2012, **186**, 450–457, DOI: 10.1164/rccm.201203-0444OC.

11 A. Zacharasiewicz, N. Wilson and A. Bush, Dilution of respiratory solutes in exhaled condensates, *Am. J. Respir. Crit. Care Med.*, 2003, **167**, 663–669, DOI: 10.1164/ajrccm.167.5.957.

12 Z. Xu, F. Shen, X. Li, Y. Wu, Q. Chen, X. Jie and M. Yao, Molecular and microscopic analysis of bacteria and viruses in exhaled breath collected using a simple impaction and condensing method, *PLoS One*, 2012, **7**, e41137, DOI: 10.1371/journal.pone.0041137.

13 C. F. Fronczek and J. Y. Yoon, Biosensors for monitoring airborne pathogens, *J. Lab. Autom.*, 2015, **20**, 390–410, DOI: 10.1177/2211068215580935.

14 K. S. Rizi, E. Aryan, Z. Meshkat, G. Ranjbar, M. Sankian, K. Ghazvini, H. Farsiani, H. R. Pourianfar and M. Rezayi, The overview and perspectives of biosensors and *Mycobacterium tuberculosis*: a systematic review, *J. Cell. Physiol.*, 2020, **236**, 1730–1750, DOI: 10.1002/jcp.30007.

15 J. Ma, M. Du, C. Wang, X. Xie, H. Wang and Q. Zhang, Advances in airborne microorganisms detection using biosensors: A critical review, *Front. Environ. Sci. Eng.*, 2021, **15**, 47, DOI: 10.1007/s11783-021-1420-8.

16 J. J. Mcdevitt, P. Koutrakis, S. T. Ferguson, J. M. Wolfson, M. P. Fabian, M. Martins, J. Pantelic and D. K. Milton, Development and performance evaluation of an exhaled-breath bioaerosol collector for influenza virus, *Aerosol Sci. Technol.*, 2013, **47**, 444–451, DOI: 10.1080/02786826.2012.762973.

17 I. Lee, Y. Seok, H. Jung, B. Yang, J. Lee, J. Kim, H. Pyo, C. S. Song, W. Choi, M. G. Kim and J. Lee, Integrated bioaerosol sampling/monitoring platform: field-deployable and rapid detection of airborne viruses, *ACS Sens.*, 2020, **5**, 3915–3922, DOI: 10.1021/acssensors.0c01531.

18 N. R. D. Sousa, N. Sandström, L. Shen, K. Håkansson, R. Vezozzo, K. I. Udekwu, J. Croda and A. G. Rothfuchs, A fieldable electrostatic air sampler enabling tuberculosis detection in bioaerosols, *Tuberculosis*, 2020, **120**, 101896, DOI: 10.1016/j.tube.2019.101896.

19 J. Ma, M. Du, C. Wang, X. Xie, H. Wang, T. Li, S. Chen, L. Zhang, S. Mao, X. Zhou and M. Wu, Rapid and sensitive detection of *Mycobacterium tuberculosis* by a enhanced nanobiosensor, *ACS Sens.*, 2021, **6**, 3367–3376, DOI: 10.1021/acssensors.1c01227.

20 J. Ma, G. Jiang, Q. Ma, M. Du, H. Wang, J. Wu, C. Wang, X. Xie, T. Li, S. Chen, L. Zhang and M. Wu, Portable immunosensor directly and rapidly detects *Mycobacterium tuberculosis* in sputum, *Anal. Methods*, 2022, **14**, 438–448, DOI: 10.1039/D1AY01561C.

21 L. Wang, W. Qi, Y. Liu, D. Essien and J. Lin, Recent advances on bioaerosol collection and detection in microfluidic chips, *Anal. Chem.*, 2021, **93**, 9013–9022, DOI: 10.1021/acs.analchem.1c00908.

22 V. Sahore, M. Sonker, A. V. Nielsen, R. Knob, S. Kumar and A. T. Woolley, Automated microfluidic devices integrating solid-phase extraction, fluorescent labeling, and microchip electrophoresis for preterm birth biomarker analysis, *Anal. Bioanal. Chem.*, 2018, **410**, 933–941, DOI: 10.1007/s00216-017-0548-7.

23 D. Chen, W. A. Bryden and M. Mcloughlin, A novel system for the comprehensive collection of nonvolatile molecules from human exhaled breath, *J. Breath Res.*, 2020, **15**, 016001, DOI: 10.1088/1752-7163/abba87.

24 N. Shehada, J. C. Cancilla, J. S. Torrecilla, E. S. Pariente, G. Brönstrup, S. Christiansen, D. W. Johnson, M. Leja, M. P. A. Davies, O. Liran, N. Peled and H. Haick, Silicon nanowire sensors enable diagnosis of patients via exhaled

breath, *ACS Nano*, 2016, **10**, 7047–7057, DOI: 10.1021/acsnano.6b03127.

25 M. Pan, J. A. Lednicky and C. Wu, Collection, particle sizing and detection of airborne viruses, *J. Appl. Microbiol.*, 2019, **127**, 1596–1611, DOI: 10.1111/jam.14278.

26 W. Jing, X. Jiang, W. Zhao, S. Liu, X. Cheng and G. Sui, Microfluidic platform for direct capture and analysis of airborne *Mycobacterium tuberculosis*, *Anal. Chem.*, 2014, **86**, 5815–5821, DOI: 10.1021/ac500578h.

27 F. Shen, M. Tan, Z. Wang, M. Yao, Z. Xu, Y. Wu, J. Wang, X. Guo and T. Zhu, Integrating silicon nanowire field effect transistor, microfluidics and air sampling techniques for real-time monitoring biological aerosols, *Environ. Sci. Technol.*, 2011, **45**, 7473–7480, DOI: 10.1021/es1043547.

28 H. Shen, F. Qu, Y. Xia and X. Jiang, Straightforward and ultrastable surface modification of microfluidic chips with norepinephrine bitartrate improves performance in immunoassays, *Anal. Chem.*, 2018, **90**, 3697–3702, DOI: 10.1021/acs.analchem.7b05186.

29 H. G. Wiker and M. Harboe, The antigen 85 complex: a major secretion product of *Mycobacterium tuberculosis*, *Microbiol. Rev.*, 1992, **56**, 648–661, DOI: 10.1016/0882-4010(92)90015-G.

30 K. S. Khaertynov, A. R. Valeeva, A. V. Ivanov, M. N. Mukminov, N. G. Urazov, I. M. Khaertynova, N. M. Aleksandrova, A. V. Moskvicheva, M. A. Efimova, R. M. Akhmadeev, E. S. Samigullina, A. A. Nabatov and E. A. Shuralev, Extraction and serological properties of *Mycobacterium* cell surface and excreted proteins, *Bionanoscience*, 2017, **8**, 459–466, DOI: 10.1007/s12668-017-0492-1.

31 V. Krivitsky, M. Zverzhinetsky and F. Patolsky, Antigen-dissociation from antibodymodified nanotransistor sensor arrays as a direct biomarker detection method in unprocessed biosamples, *Nano Lett.*, 2016, **16**, 6272–6281, DOI: 10.1021/acs.nanolett.6b02584.

32 S. W. Li, A. V. Nguyen and Z. Q. Sun, Stochastic induction time of attachment due to the formation of transient holes in the intervening water films between air bubbles and solid surfaces, *J. Colloid Interface Sci.*, 2020, **565**, 345–350, DOI: 10.1016/j.jcis.2020.01.027.

33 C. Marie-Desvergne, M. Dubosson, L. Touri, E. Zimmermann, M. Gaude-Môme, L. Leclerc, C. Durand, M. Klerlein, N. Molinari, I. Vachier, P. Chanez and V. C. Moss, Assessment of nanoparticles and metal exposure of airport workers using exhaled breath condensate, *J. Breath Res.*, 2016, **10**, 036006, DOI: 10.1088/1752-7155/10/3/036006.

34 A. M. Giuliodori, F. D. Pietro, S. Marzi, B. Masquida, R. Wagner, P. Romby, C. O. Gualerzi and C. L. Pon, The cspA mRNA is a thermosensor that modulates translation of the cold-shock protein CspA, *Mol. Cell*, 2010, **37**, 21–33, DOI: 10.1016/j.molcel.2009.11.033.

35 C. Imashiro, M. Hirano, T. Morikura, Y. Fukuma, K. Ohnuma, Y. Kurashina, S. Miyata and K. Takemura, Detachment of cell sheets from clinically ubiquitous cell culture vessels by ultrasonic vibration, *Sci. Rep.*, 2020, **10**, 9468, DOI: 10.1038/s41598-020-66375-1.

36 P. K. Chanda, A. Bandhu, B. Jana, R. Mondal, T. Ganguly, K. Sau, C. Y. Lee, G. Chakrabarti and S. Sau, Characterization of an unusual cold shock protein from *Staphylococcus aureus*, *J. Basic Microbiol.*, 2011, **50**, 519–526, DOI: 10.1002/jobm.200900264.

37 I. C. Duru, A. Ylin En, S. Belanov, A. V. Pulido and P. Auvinen, Transcriptomic time-series analysis of cold- and heat-shock response in psychrotrophic lactic acid bacteria, *BMC Genomics*, 2021, **22**, 1–16, DOI: 10.21203/rs.3.rs-34513/v1.

38 C. Gessner, H. Kuhn, H. J. Seyfarth, H. Pankau, J. Winkler, J. Schauer and H. Wirtz, Factors influencing breath condensate volume, *Pneumologie*, 2001, **55**, 414–419, DOI: 10.1055/s-2001-16947.

39 K. P. Fennelly, J. W. Martyny, K. E. Fulton, I. M. Orme, D. M. Cave and L. B. Heifets, Cough-generated aerosols of *Mycobacterium tuberculosis*, *Am. J. Respir. Crit. Care Med.*, 2004, **169**, 604–609, DOI: 10.1164/rccm.200308-1101OC.